Date of publication xxxx 00, 0000, date of current version xxxx 00, 0000.

Digital Object Identifier 10.1109/ACCESS.2017.DOI

A Dynamic Behavior-Based Bulk Power System Event Signature Library with Empirical Clustering

KOJI YAMASHITA[1], (Member, IEEE), BRANDON FOGGO[1], (Member, IEEE), XIANGHAO KONG[1], (Student Member, IEEE), YUANBIN CHENG[1], (Student Member, IEEE), JIE SHI[1], (MEMBER, IEEE), NANPENG YU[1], (Senior Member, IEEE).

[1]Electrical and Computer Engineering, University of California Riverside, Riverside, CA, 92521 USA (e-mail: [kyamashi@, brandon001@, nyu@ece., xkong016@, ychen871@, and jshi@]ucr.edu)

Corresponding author: Koji Yamashita (e-mail: kyamashi@ucr.edu).

ABSTRACT The grid reinforcement, advanced grid stabilizing systems, and inverter-interfaced loads have varied power system dynamics. The changing trends of various dynamic phenomena need to be scrutinized to ensure future grid reliability. A dynamic behavior-based event signature library of phasor measurement unit (PMU) data has great potential to discover new and unprecedented event signatures. This paper presents an event signature library design that further defines more granular event categories within the major event categories (e.g., frequency, voltage, and oscillation events) provided by electric utilities and regional transmission organizations. The proposed library design embraces a supervised machine learning approach with a deep neural network (DNN) model and manually-generated labels. The input of the model uses representative PMUs that evidently express dominant event signatures. The performance of the event categorization module was evaluated, via information entropy, against labels generated automatically from clustering analyses. We applied the event signature library design to two years of over 1000 actual events in the bulk U.S. power system. The module obtains remarkable event discrimination capability.

INDEX TERMS Classifier, clustering, deep neural network, event library, power system, PMU, residual network, event signature.

I. INTRODUCTION

POWER system abnormal events have usually been categorized based on stability [1] or power outage scale [2], [3]. These captured grid events have been listed according to protective relay logs, system operator's switching maneuver logs, and monitoring system logs. The monitoring system-based event detection has moved to fruition thanks to the disseminating grid sensors, such as the phasor measurement unit (PMU) [4], [5], frequency monitoring network (FNET) [6], and digital fault recorder (DFR) [7]. Specifically, a *forced* oscillation event across the Eastern Interconnection (EI) in the U.S. in Jan. 2019 [8] turned engineers' significant attention to the need for new event feature extractions with localization through grid-wide measurement devices [9].

Such prosperity of the PMU application studies also triggers the industry's new interest in event signature datasets. Specifically, the Department of Energy in the U.S. launched a new working group, titled "Grid Signature Library User Group" in March 2022, inviting both academia (universities and research institutes) and the industry (transmission system operator (TSO), regional system operator (RTO), manufacturers, and PMU vendors). The major goal is to establish a solid and reliable grid event signature library based on the real-world grid events measured by PMUs and event logs recorded by TSOs/RTOs (https://darknet-01.ornl.gov/apps/siglib).

The North American Electric Reliability Corporation (NERC) reliability coordinator has dedicated efforts to fulfilling sufficient energy security, by regulating severe incident report forms with the definition of its severity level [2], [3]. Tracking the transition of the conventional event signature is one of the most efficient ways to develop countermeasures to the rapid change in grid performance due to the RES. However, such event reports are not entirely sufficient in scrutinizing the event signature transition mainly because:

- The current grid event categorization primarily relies on the protective relay operations, including warning/alert system operations,
- The aforementioned event categorization is limited to the large-category level (e.g., frequency, voltage, and oscillation events), and
- The smaller category is determined by TSOs/RTOs with their own criteria.

The dynamic behavior-based categorization in conjunction with unified criteria could be one of the promising approaches for enhancing the current event signature database to track the above-mentioned signature transition from the reliability council's point of view as well as TSO/RTO's perspectives.

In light of the above, an event signature library design that further defines more granular event categories within the major event categories provided by TSOs/RTOs has been developed. The proposed library design embraces a supervised machine learning approach with a deep neural network (DNN) model and empirical labels.

The core of the event signature library (hereafter, we call this the event library) is a power system event classification module. The existing researches in event classification comprise data-driven methods and model-based methods [10]–[28]. The former is predominant. Data-driven methods are grouped into two approaches:

1) Supervised learning, such as cost-sensitive weighting and imbalance-reversed bagging [18], cascading failures detection using convolutional neural networks [20], time-frequency representation feature extraction in the extreme learning machine [16], cluster-based sparse coding [17], and diffusion kernel density estimation with deep neural networks [19],
2) Unsupervised learning, such as moving window principal component analysis [22], the Teager Kaiser energy operator [23], a brown measure based spectral distribution analysis [25], nonnegative sparse event unmixing [21], continuity driven learning [26], the waveshape similarity metric [24], DBscan [27], and Koopman mode analysis [28].

The first data-driven approach based on supervised learning requires labeled data. However, no research deals with a wide variety of dynamic behaviors in a holistic manner, and the choice of labels differs from article to article, with different perspectives shown below:

- Electric quantity (active power, reactive power, voltage) [26]–[28],
- Fault (single-line-to-ground, line-to-line, 3-phase) [26], [29], [30],
- Equipment trip (transmission, bus, generator, load) [17], [21]–[23], [30], [31].

As shown above, the employed label is mainly generated from the protective relay operation log and warning system log instead of dynamic behavior-based distinction. Therefore, those labels are not exploited for our dynamic behavior-based event library for practical purposes.

The second data-driven approach based on unsupervised learning requires preassigned large-category dynamic aspects to be studied, i.e., it needs to narrow down the targeted event signature. This approach cannot accurately handle the combined event signatures, such as the mixture of voltage and frequency events, specifically when multiple events occur simultaneously. Although subsequent event classifications have been studied [17], [21]–[23], only frequency signals were exploited. Because many combined events have occurred in the actual grid, unsupervised learning is not suited for the event library design.

Our proposed event library leverages three predominant signals among four signals (voltage, frequency, active power, and reactive power), specifically designed to identify the following simultaneous events:

- Voltage event and frequency event,
- Voltage event and oscillation event,

and the following distinctive detailed signatures:

- Frequency event with and without frequency transients,
- Voltage event with and without slow voltage recovery,
- Inter-area oscillation and local oscillation, including sub-synchronous oscillation.

The developed event library is designed with the real-world grid-wide event data in 2016-2017 in the U.S. recorded by PMUs, and the corresponding event labels generated by electric utilities and TSO/RTOs with further refinement by Pacific Northwest National Laboratory (PNNL) [32]. However, the quality of not only PMU data [33] but also labels [34] does not always suffice. Specifically, the following inconsistencies or incompleteness in the provided labels are prone to deteriorate the event log quality:

- Power equipment and power system phenomena are categorized in the same group/level (e.g., transformer and oscillation).
- Cause and effect are categorized in the same group/level (e.g., equipment failure and line trip).
- Only one event of subsequent multiple events is listed (e.g., generator tripping is only indicated although a line fault occurred before the tripping).
- A part of the phenomena is only listed (e.g., frequency drop behavior is only depicted, although power swing oscillation was also observed throughout the event).

Due to the aforementioned event label quality issues, the only large-category label becomes capitalized as the starting

point for our event library. Then, small-category labels are manually specified by subject-matter experts reviewing individual, real-world events. The onus is on engineers to prove that these refinements have value. Such proof is one of the primary goals of this paper. However, very little research in the machine learning community exists on the justification of labels themselves. Thus, motivated by the widely used inception scores utilized in deep generative models [35], we have decided to use an external classifier as a means of determining label value. The idea is that if a classification module trains on these labels, then when a new event occurs, that event should be assigned to just one of these labels without confusion. To this end, the Shannon entropy of predictions is employed as a quality of measure. This entropy is performed by an external deep neural network (DNN) on future events, relative to the events used to train the model. This quality measure yields the additional benefit of allowing the user to quickly identify a new/unprecedented event label to be added.

The developed event library is capable of displaying the average dynamic characteristics for each category. Although examples of event signatures are showcased in many textbooks, scholarly articles, and technical reports, the standard dynamic responses for individual event signatures are not mandated in a systemic manner. Therefore, illustrating the representative waveforms for each event category is beneficial for the engineer's educational purposes.

It is emphasized that the event signature library is different from the event classification/identification. Generally, the event classifier attempts to categorize all events into a preassigned label. However, the event library may collect or extract events of interest only. In other words, unconventional events may also be present in the event library. The main contributions of this paper are:

- To detect exceptionally rare event types or discover unprecedented event types, through which TSOs/RTOs can recognize how rare the event is and we may suggest adding a new classification label
- To serve smaller event categories, such as
  - -- combined (e.g., voltage and frequency) events,
  - -- voltage events with/without slow voltage recovery,
  - -- oscillation events with/without local-area oscillation,

  which appends a more detailed view to the current event report that TSOs/RTOs prepare and more granular event labels for machine learning research studies,
- To clarify the representative signature for each event type, which may be embraced for research and education purposes,
- To demonstrate that the manually created labels showed a better classification performance with the event classifier compared to automatically-created labels, which justifies the necessity of domain expert's knowledge for accurate event signature labels.

The rest of the paper is organized as follows: Section II clarifies how to capitalize on the event library design, Section III illustrates how to establish the event library design, Section IV justifies the performance of the event library via case studies, Section V manifests future work.

II. ARCHITECTURE OF EVENT SIGNATURE LIBRARY DESIGN

This section articulates how the event library design enhances the event report that the reliability coordinator currently requires. Then, it reveals how to establish the event classifier module in the event library.

A. FLOW OF EVENT SIGNATURE LIBRARY DESIGN

The event report typically consists of the cause, impact, and action taken [36]. Both the power equipment loss or failure and the excursions of electric quantities, such as voltage and frequency, are the dominating criteria for declaring disruptive events in the event report [2] (treated as high-level labels).

Figure 1 overviews the scope of the event library design, contrasting the aforestated event report. The event library assumes that the high-level (large-category) labels are known through the event report. Low-severity events, such as fault type and affected power equipment with its location, may be recorded by electric utilities and TSOs/RTOs spontaneously. However, they cannot be leveraged on their own for the event library due to the deficient consistency of the low-level (small-category) labels between TSOs/RTOs. It is emphasized that *PMU locations are not disclosed* by the PNNL.

The event library is separately designed depending on high-level (large-category) labels. The event library design starts to function once the high-level (large-category) label and PMU data are provided as input. Then, the classifier module in the event library design identifies the low-level (small-category) labels for the designated high-level label. Specifically, the established classifier module calculates the probabilities of individual labels/clusters, and the label with the highest probability is treated as the identified label. The identified low-level label is scrutinized with the information entropy. If the probability is not concentrated on a particular label, the selected low-level label is rejected, and the possible discovery of a new event type will be manually examined.

B. CLASSIFIER MODULE ESTABLISHMENT PROCESS

The classifier module in the event library design is established through supervised learning algorithms. The overall procedure for establishing the classifier module is illustrated in Fig. 2.

Training the module requires corresponding labels (i.e., low-level event types) as well as PMU data. These labels can be generated manually or automatically. Experienced engineers can prepare the labels empirically by perceiving a significant event signature, whereas clustering techniques can be used for automation. This paper creates automatic labels via the K-means clustering with dynamic time warping (DTW) chosen as its distance metric. We will treat these automatically-generated labels as the baseline module. The performance of this baseline module is compared with the

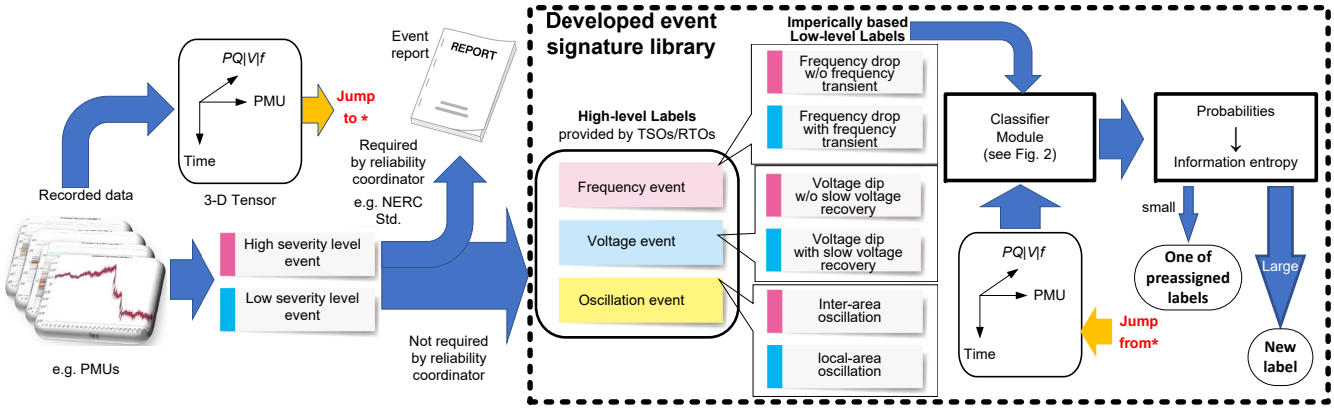

FIGURE 1. Conventional high-level event report procedure and new low-level event report procedure (with proposed event signature library).

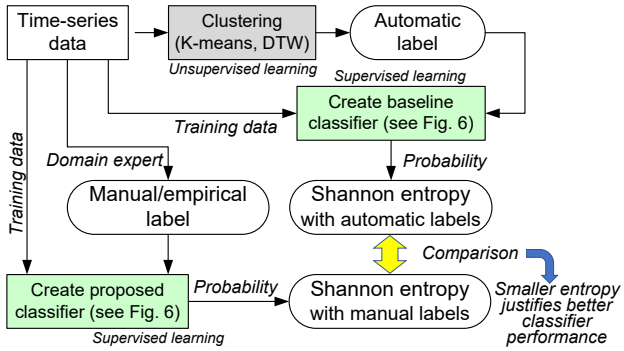

FIGURE 2. Procedure of establishing classifier module in event library design.

performance of the manually-generated labels. The aforementioned information entropy is employed for the comparison. Specifically, the classifier module with the smaller mean entropy (taken over all the samples) has labels that are more easily distinguishable from each other by their corresponding trained classifier and will therefore be considered the better set of labels.

III. ESTABLISHMENT OF EVENT SIGNATURE LIBRARY DESIGN

This Section embodies the event signature library design, showcasing the preprocessing, manually-generated label, electric quantity selection, DNN modeling, and event label scrutiny.

A. PREPROCESSING

PMU data contains various types of imperfections:

- Erroneous and missing data
- Data with low signal to noise ratios (SNR)
- Oscillatory signals

Various techniques have been studied to cope with the low-quality data [37], [38] and are categorized into two groups:

1) Removing PMUs that have low-quality data
2) Replacing missing data with plausible data

The first group improves data reliability, but reduces the available data volume. The second group increases the available data, but decreases the data integrity. As the volume of data grows, the latter becomes less critical.

Not all PMU data and not all the events properly exhibit noticeable signatures relative to the particular phenomenon. Extracting a few remarkable signals from hundreds of PMUs is more crucial than leveraging ample PMUs (some of which could have low-quality data). Furthermore, the preprocessing speed is not necessarily a problem because TSOs/RTOs are permitted to spend anywhere from a few hours [39] up to a month [2] generating their event reports.

1) Standard deviation-based thresholds

NERC and IEEE standards specify normal operation ranges in voltage and frequency at steady-state [40]. However, such normal ranges cannot be leveraged as threshold values to identify malfunctioning PMUs because this would eliminate important event data violating said normal range. Instead, we must note that malfunctioning PMUs, including out-of-service PMUs, present values outside of the normal range continuously or intermittently. We thus filter out PMUs only when their standard deviation exceeds a threshold - where the standard deviation is calculated over a time period exceeding that of a typical event. After reviewing over 700 events with 187 PMUs, the following standard deviation thresholds are leveraged, as shown in Table 1.

As shown in Table 1, threshold values consist of lower thresholds and upper thresholds. Lower thresholds are primarily determined for the purpose of differentiating the nearly constant electric quantities due to out-of-service or malfunctioning PMUs from the ambient electric quantities, such as active power. Upper thresholds are primarily determined for the purpose of excluding out-of-range or erroneous measurements with sufficient margins. The fundamental criteria of lower thresholds were determined based on probabilities of recorded standard deviations of electric quantities in the EI.

TABLE 1. Thresholds for Excluding Malfunctioning PMUs

Standard deviation	Lower limit	Upper limit
Role of thresholds	1) Remove low resolution signal** 2) Remove out-of-service PMU	1) Remove oscillatory signal 2) Remove low S/N signal
Active power, P pu*	0.003	30
Reactive power, Q pu*	0.003	30
Voltage, V pu	0.0001	0.02
Frequency, F Hz	0.0012	0.2

*: per unit value calculated with system complex power base of 100 MVA
**: data with small effective digits and data with no change for a second

a: Lower Threshold:

Thresholds of active power, P, and reactive power, Q, were selected between the two modes of the P/Q histogram at 0∼5th percentile: 1) the histogram of the ambient P/Q fluctuation, and 2) the histogram of the erroneous P/Q signals (see Fig. 3). It is noted that P and Q standard deviations are similarly distributed. Therefore, we may employ the same lower thresholds of 0.003 for P and Q.

Similarly, the voltage magnitude, V, also contains two modes on the histogram at 0∼5th percentile. Because the V threshold is extremely small, we rounded the V threshold to 0.0001 (i.e., from 0.00006 to 0.0001).

However, the frequency, F, possesses only one mode on the histogram at 0∼5th percentile. Because all the other electric quantities have the threshold at the 1st percentile, the same 1st percentile was employed for the F threshold, i.e., 0.0012 Hz.

b: Upper Threshold:

The active power flow can potentially show immediate change from the initial power flow to zero following grid events. This power flow change would reach a few GW. Not to exclude significant grid events with such large power changes, 3 GW/Gvar (3000 MW/Mvar) was selected as the threshold, which corresponds to 9 GW/Gvar of power deviation (3 times the standard deviation covers the sojourn rate of 99.7%).

The transmission voltage is generally in the continuous operation range of 0.05∼0.10 pu relative to the nominal voltage (e.g., 1.0∼1.1 pu for 500 kV and 0.95∼1.05 for 69∼345 kV in the PJM). Considering the 0.02 pu margin and assuming that the voltage peak-to-peak is equal to 6 times the standard deviation of voltage, the threshold of 0.02 pu was selected, which corresponds to 0.12 pu (= 0.1 pu + 0.02 pu margin) of the peak-to-peak voltage fluctuation.

The frequency nadir in the bulk power systems (such as the EI and WECC) is generally less than 0.5 Hz that is used as the lower operating limit in the PJM. Ensuring the 0.1 Hz margin and assuming that the frequency deviation is equal to 3 times the standard deviation of frequency, the threshold of 0.2 Hz was selected, which corresponds to 0.6 Hz (= 0.5 Hz + 0.1 Hz margin) of the frequency deviation.

TABLE 2. Empirical Low-level Label of Frequency Event

Label	Frequency change	Voltage sag	Remark
1	No frequency drop	No	no-event
2	Large transient	Tiny/no	
3	Large transient	Large	following voltage event
4	Tiny or no transient	Tiny/no	

2) K-shape clustering

Threshold values in Table 1 are not entirely effective in removing oscillatory signals and low SNR measurements because the amplitude of those signals varies widely depending on location, power system configuration, and operation conditions. A clustering technique, called K-shape clustering [41], is employed to take out these missed signals. Among a wide variety of clustering methods, K-shape clustering is adopted because it is both scale and shift-invariant.

K-shape clustering uses a shape-based distance (SBD), as shown in Eq. (1). The vectors, $\boldsymbol{X}$ and $\boldsymbol{Y}$, denote two time-series data. The function, CC, denotes a cross-correlation that is widely-used as the similarity index. The variable, SBD, searches for the maximal inner product with the normalized cross-correlation of the two time-series data.

$$SBD(\boldsymbol{X},\boldsymbol{Y}) = 1 - \max_{w}\left(\frac{CC_w(\boldsymbol{X},\boldsymbol{Y})}{\sqrt{R_0(\boldsymbol{X},\boldsymbol{X})\cdot R_0(\boldsymbol{Y},\boldsymbol{Y})}}\right) \quad (1)$$

where,

$$CC_w(\boldsymbol{X},\boldsymbol{Y}) = R_{w-m}(\boldsymbol{X},\boldsymbol{Y}), w \in \{1,2,...,2m-1\}$$

$$R_k(\boldsymbol{X},\boldsymbol{Y}) = \begin{cases} \Sigma_{l=1}^{m-k} x_{l+k}\cdot y_l, k \geq 0 \\ R_{-k}(\boldsymbol{Y},\boldsymbol{X}), k < 0 \end{cases}$$

K-shape clustering effectively distinguishes the event signature to be observed from oscillatory behavior that is irrelevant to the targeted event signature. Fig. 4 shows an example of a frequency event with K-shape clustering. Event timings are assumed to be known for each event and adjusted to 600 in this figure. This figure shows that the first cluster includes a noisy signal, and the third cluster indicates inter-area oscillation. In this example, the second cluster is the best cluster to extract prominent frequency event signatures. It is noted that K-shape clustering is embraced only for frequency events and voltage events.

B. EMPIRICAL (MANUALLY-GENERATED) LABELS

As described earlier, high-level (large category) labels provided by the PNNL, consist of three categories:

1) Frequency-related event
2) Voltage-related event
3) Oscillation event

Based on the rigorous review of several hundreds of those events, low-level (small category) labels, are established for each category (see Tables 2, 3, and 4). Those low-level labels nearly cover the labels listed in a similar research study using the same datasets [34], [42]. It is noted that domain experts

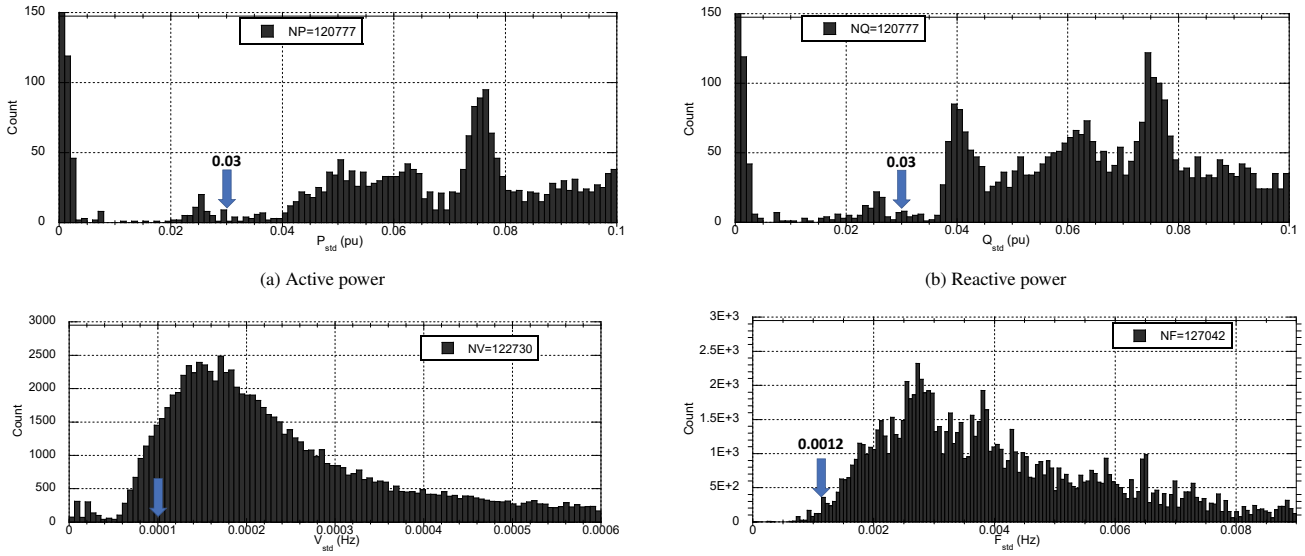

(a) Active power (b) Reactive power

(c) Voltage (d) Frequency

FIGURE 3. Histograms of standard deviations of active power, reactive power, voltage, and frequency.

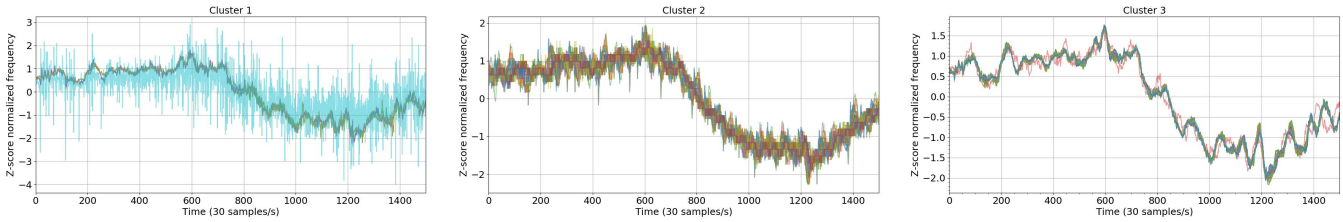

FIGURE 4. Example result of K-shape clustering for frequency using Z-score normalization.

TABLE 3. Empirical Low-level Label (Small-category Label) of Voltage Event

Label	Voltage deviation/drop	Reactive power deviation	Slow voltage recovery	Subsequent voltage dynamics	Remarks
1	Less than 0.5%	N/A	Imperceptible	No	Non-event and nearly non-event
2	N/A	N/A	Perceptible	Yes	Subsequent dynamics with voltage recovery
3	N/A	N/A	Clearly perceptible	No	Pronounced slow voltage recovery
4	Greater than 3.0%	Greater than 30 pu	Imperceptible	No	Large voltage drop
5	Greater than 0.5%	Less than 100 pu	Imperceptible	No	Medium-scale voltage drop with no slow voltage recovery

derived the listed labels shown in references [34], [42]. The cause of events is out-of-scope for the low-level label because of the deficiency of relevant information, e.g., no information on the placement of PMUs, which could deteriorate the low-level label accuracy. Identifying the affected power equipment is also excluded in this study for the same reason.

1) Frequency Event

Frequency event signatures are differentiated by the presence of voltage events (label 3) and significant voltage phase jumps (labels 2 and 3). Label 1 is assigned for non-event signatures.

2) Voltage Event

Voltage event signatures are distinguished by the presence of slow voltage recovery (labels 2 and 3), significant voltage dip (label 4), and subsequent voltage sag (label 2). Label 1 is allocated to non-event signatures.

3) Oscillation Event

Oscillation event signatures are separated by the presence of voltage events (label 2) and have two different participation rates of local area oscillations (labels 1 and 3). The inter-area oscillation is assumed to be observed in the oscillation event explicitly. Signals with weak inter-area oscillation are treated as non-events (label 5).

C. ELECTRIC QUANTITY SELECTION

Prominent signals emerge in specific electric quantities. PMU data captures voltage and current data as time-domain phasor information, allowing us to derive active power, reactive power, frequency, and rate of change of frequency. The

TABLE 4. Empirical Low-level Label of Oscillation Event

Label	Voltage dip	High-frequency component	Low-frequency component	Remark
1	N/A	Weak	Strong	Low participation of local-area oscillation
2	Large	N/A	Strong	Voltage event with inter-area oscillation
3	N/A	Strong	Strong	High participation of local-area oscillation
4	Small	No	Strong	Switching event with inter-area oscillation
5	No	No	Weak	Non-event

TABLE 5. Used Electric Quantity for Each Event Type

Event	Active power (P)	Reactive power (Q)	Voltage ($\|V\|$)	Frequency (F)
Frequency	X		X	X
Voltage	X	X	X	
Oscillation	X	X	X	

available electric quantities should be capitalized to acquire a better classifier performance in the event library. The electric quantities selected for each event type are shown in Table 5. Each type of large category label ignores one type of data.

Tiny reactive power changes caused by compensators, or tap changers, are generally irrelevant to frequency dropping/rising behavior. Therefore, reactive power is skipped for frequency events. In the same manner, frequency is excluded for voltage events because frequency fluctuation does not usually affect voltage events. Furthermore, frequency is also omitted for oscillation events. The frequency resolution is not always high enough to capture high-frequency oscillations, which would worsen the event library performance, especially when the frequency deviation is nearly zero.

D. SELECTION OF PMUS

The numbers of valid PMUs for the event signature library in the EI and WECC are 187 and 43, respectively. Although numerous PMUs are available for the event library, only a few PMUs significantly exhibit the behavior of some events. Influential factors vary depending on the event type. In this work, we train our models on a fixed number of PMUs which have the largest amount of set criteria. These criteria and the number of selected PMUs vary by high-level (large-category) event types.

Voltage events use three PMUs and voltage dip magnitude as criteria. In other words, the PMUs that have the first, second, and third-largest voltage deviations are extracted as the top 3 PMUs for voltage events. As the slow voltage recovery is more remarkable when the voltage dip increases, this factor works well not only for label 4 but also for labels 2 and 3 in Table 3. Considering that voltage events are generally local incidents, the number of selected PMUs is limited to three for voltage events.

On the other hand, frequency events may be treated as grid-wide incidents. Therefore, the number of selected PMUs is raised to five for frequency events. The transient/immediate frequency change that is observed right when the frequency event occurs is used as a criterion. This criterion is a good indicator since transient frequency behavior corresponds with the significant power flow change and voltage phase jump. Therefore, the top 5 PMUs with this criterion are highly likely to be the top 5 PMUs that have a notable voltage (magnitude) deviation. That means this criterion is effective in capturing the dominant behavior of label 3 as well as label 2 in Table 2.

Oscillation events exhibit quite a different spatiotemporal aspect compared to frequency and voltage events. The oscillation event occurrence is recognized using the frequency domain analysis (fast Fourier Transform-based spectrum analysis). The adoption condition of PMUs for oscillation events is illustrated in Fig. 5. Three AND conditions are employed to properly extract PMUs that contain oscillatory signals, excluding noisy signals and periodically dropped out (square wave) signals. This procedure is applied to active power, reactive power, voltage, and frequency, respectively, and append the PMU that satisfies the aforementioned three conditions for each oscillation event.

Because the significant PSD that is over *PSD0* in Fig. 5 needs to contain $0.2 \sim 10$ Hz frequency components, the number of selected PMUs with the oscillatory behavior is widely distributed from event to event in the range of 0 and 70 in the EI. Therefore, PMUs that represent conspicuous oscillatory behavior are manually identified individually, using frequency domain analysis. In other words, the number of selected PMUs for oscillation events is variable. The low and high-frequency components in Table 4 are defined as follows, referring to [43], [44]:

High-frequency: Mode oscillation range of 1-10 Hz
Low-frequency: Mode oscillation range of 0.15-1 Hz

According to the NERC guideline, high-frequency oscillation is again categorized into two mode oscillations: the local-area oscillation and sub-synchronous/converter-driven oscillation. Due to the limited volume of available data for the latter oscillation, this paper integrates these two mode ranges into a single category, called high-frequency oscillation. It is noted that the number of significant digits is 15 due to the double-precision data, which enables us to select the top 3/5 PMUs without the same ranking.

E. TRAINING DATASET GENERATION VIA AUGMENTATION MEASURE

Training datasets are generated using 121 real frequency events and 189 real voltage events in the EI, which requires the data augmentation to increase the number of instances we train on. There are two measures to augment the PMU measurement for training datasets: using the detailed dynamic bulk power system model that TSOs/RTOs own, and generating the realistic synthetic PMU data using the real PMU measurement. However, such models are not available/disclosed, and such synthetic data generation is still in

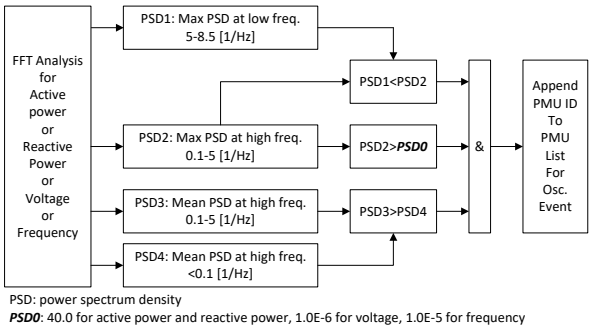

FIGURE 5. PMU selection procedure for oscillation events.

TABLE 6. Training Dataset (Number of Event/Number of Sample)

Event type	Label 1	Label 2	Label 3	Label 4	Label 5
Frequency	18/2250	43/5375	18/2250	42/5250	N/A
Voltage	34/918	22/594	45/1215	34/918	54/1458
Oscillation	3263*	6350*	777*	5332*	1891*

*: Number of samples only

the research stage [45]. Unlike the random horizontal flip, random resize crop, and random rotation widely applied for images, the distilled PMUs are mixed and matched across data types. For example, if three PMUs are extracted from an event, and PQV data is used, then one of the augmented training samples consists of the P data from the first PMU, the Q data from the second, and the V data from the third. All such enumerations are used, multiplying the number of training points by a factor of n^r, where n and r denote the number of extracted PMUs per event and the number of employed electric quantities, respectively.

It is evident that the enumeration exponentially increases with the number of extracted PMUs. Because the number of these PMUs for a specific oscillation event is large, e.g., 70, the enumeration becomes huge. This causes a too-heavy weight for a particular event among the training dataset, which could deteriorate the dataset quality. Therefore, the augmentation strategy above is applied for oscillation events, only when the number of selected PMUs is no greater than 3. Nevertheless, since the number of PMUs exhibiting oscillatory event signatures is naturally high, 17613 total training datapoints can be obtained for this event type (see Table 6).

F. DEEP CONVOLUTIONAL NEURAL NETWORK MODEL

The proposed categorization module consists of two components: the encoder and the classifier modules (see Fig. 6). The encoder transforms the input data into representative features. The feature maps are then fed into the classifier, which identifies the high-probability (i.e., predominant) grid event signature. The input $PQ|V|f$ tensors are arranged using the selected PMUs described in Section III-D. A widely-used deep convolutional neural network (CNN), the second version of ResNet-50 (ResNet-50 V2) [46], is embraced as the key building block of the encoder. The ResNet50 V2

TABLE 7. Hyperparameter of Categorization Module

Hyperparameter	Group	Category	Value/function
Momentum	SGD	Optimizer	0.95 (Freq) 0.97 (Volt) 0.99 (Osc.)
Learning rate	SGD	Optimizer	0.0020 (Freq) 0.0025 (Volt) 0.0020 (Osc.)
Dropout rate	Dropout layer	Model structure	Not used
Function type	—	Activation function in classifier	Softmax

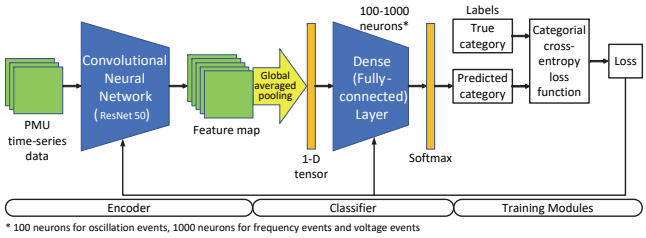

FIGURE 6. Categorization module in event signature library.

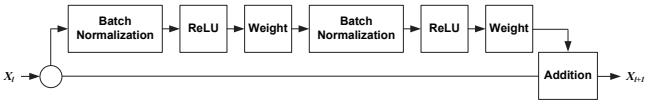

FIGURE 7. Block level architecture of ResNet 50 V2.

model has achieved excellent success on some classification tasks, especially for images.

The block-level architecture of ResNet-50 V2 is illustrated in Fig. 7. The classifier is designed as one dense layer of 100-1000 neurons with a softmax activation function. Stochastic gradient descent (SGD) with the momentum is selected as the optimizer. The categorical cross-entropy loss is chosen as the loss function. Once the training session is completed, the aforementioned optimizer, loss function, and labels are no longer needed, and the established ResNet-50 model will serve as a standalone unit to identify the event signatures for the newly recorded PMU data. The leveraged hyper-parameters are summarized in Table 7.

It is noted that a different model is trained for each high-level event type (voltage, frequency, oscillation), though the structure of each model remains the same.

G. LABEL SCRUTINY

The generated categorization module outputs probabilities of all assigned event signature categories, individually expressed as $P_r(\boldsymbol{X} = x_1, x_2, ..., x_{n_{\text{cluster}}})$. The category that has the largest probability is selected as the derived event signature category. However, the obtained probabilities can be equally distributed to multiple categories. To evaluate the likelihood of the model output, the information entropy, $I(\boldsymbol{X})$, is utilized as an indicator, shown in Eq. (2). The

information entropy is tiny when a sample (i.e., an event) is classified into one particular category and becomes large when the sample is decentrally classified into multiple categories. Therefore, the mean information entropy across a validation set is scrutinized when comparing the performance of the classifier module with empirical clustering and K-means clustering.

$$I(\boldsymbol{X}) = -\sum P_r(\boldsymbol{X} = x) \cdot \log_2 P_r(\boldsymbol{X} = x) \tag{2}$$

It is also addressed that the large information entropy represents the weak similarity to any pre-assigned categories. Therefore, the large information entropy may justify that the examined event signature is unprecedented. Thus, the information entropy contributes not only to justifying the classification performance, but also to discovering an unprecedented signature that is not recognized in historical events (see Subsection IV-D).

H. REPRESENTATIVE EVENT SIGNATURE IDENTIFICATION

Once the event signature library is created, representative event signatures may be extracted for each event signature category/cluster. Several approaches can be employed. For our work, because vast quantities of data are available for each cluster, a single PMU representing the closest dynamic behavior of each *cluster centroid* is identified and treated as the representative signal for the specific event signature category/cluster. Cluster centroids, c_j, can be obtained when the objective function of K-means, J, is minimized, as shown in Eq. (3).

$$J = \sum_{j=1}^{n_{\text{cluster}}} \sum_{i=1}^{n_{\text{sample}}} \|x_i^j - c_j\|^2 \tag{3}$$

IV. CASE STUDY

The created event signature library's performance is intensively analyzed using both manually-created labels and automatically-created labels. Automatic labels are created via the K-means clustering and dynamic time warping (DTW) [47], respectively. Then, the new event signature mining performance is also examined using the Shannon entropy (information entropy) in the created event signature library. The case study was performed using the computer with the CPU of Intel Core i7-11800H, 16 GB GPU memory, and 64 GB RAM.

A. BENCHMARK ALGORITHMS

Low-level (small category) labels in our classification submodule are manually-generated by the domain expert review of over 1000 actual events in the bulk U.S. power grid. To demonstrate the utility of these labels, another set of competing labels is generated. As already described in Subsection II-B, the comparison set is created with unsupervised machine learning - specifically K-means clustering with dynamic time warping (DTW) used as a distance metric.

K-means clustering is one of the most common forms of unsupervised clustering used in practice. The method relies on a metric of the distance between two points. For time-series data, the Euclidean distance is typically the default choice. However, the Euclidean distance is neither shift-invariant nor length-scale invariant. Lacking the shift-invariance means that two remarkably similar events could be far apart if the events happen to start at different time indices. Lacking the time-scale invariance means that two very similar events could be very far apart if one of those events resolves more quickly than another.

To avoid the pitfalls of Euclidean distance, we opt to use the dynamic time warping instead. Essentially, the DTW is just a version of Euclidean distance that enumerates all possible scale and shift factors between the two time-series inputs, and outputs the shortest such distance. Its exact formula is shown in Eq. (4):

$$DTW_{\text{distance}}(\boldsymbol{X}, \boldsymbol{Y}) = \min_{\pi} \sqrt{\sum_{(i,j)\in\pi} (x_i - y_j)^2} \tag{4}$$

$$\pi = \{(0,0), ..., (i_k, j_k), ..., (m-1, m-1)\}$$

$$\begin{cases} 0 \le i_k < m, & i_{k-1} \le i_k \le i_{k-1} + 1, \\ 0 \le j_k < m, & j_{k-1} \le j_k \le j_{k-1} + 1, \end{cases}$$

where, $\boldsymbol{X}$ and $\boldsymbol{Y}$ are two different time-series composed of the elements shown below:

$$\boldsymbol{X} = \{x_0, x_1, x_2, ..., x_m\}, \quad \boldsymbol{Y} = \{y_0, y_1, y_2, ..., y_m\}$$

For a thorough comparison, we have also created a set of labels using the Euclidean distance. The labels using Euclidean distance will hereafter be called the "K-means" set of labels, and the set using dynamic time warping will be called the "DTW" set of labels.

B. COMPARISON OF PERFORMANCE OF CLASSIFIER MODULE USING K-MEANS CLUSTERING AND EMPIRICAL CLUSTERING

The performance of the classifier module with K-means labels, DTW labels, and manual (empirical) labels is illustrated in Table 8. The mean information entropy for the testing datasets is calculated individually. The testing data is all from the western electricity coordinating council (WECC) with high-level labels (i.e., frequency, voltage, and oscillation events). As the numbers of labels are four for frequency and five for voltage and oscillation events, the maximum information entropy becomes 2.00 for frequency events and 2.32 for voltage and oscillation events. The distribution of the information entropy is displayed in Fig. 8.

As shown in Table 8, the classifier module with empirical labels presents the smallest mean information entropy against its competitors, i.e., the best performance, in every case. The DTW labels present the second smallest mean information entropy for all categories.

TABLE 8. Performance of Classifier Module for Event in WECC

Approach	Frequency event			Voltage event			Oscillation event		
	1	2	3	1	2	3	1	2	3
Clustering method	Empirical clustering	K-means clustering	DTW clustering	Empirical clustering	K-means clustering	DTW clustering	Empirical clustering	K-means clustering	DTW clustering
Number of clusters (labels)	4			5			5		
Number of sample/event	1119/373			1776/592			416/ Not applicable		
Mean of information entropy	**0.170**	0.302	0.216	**0.066**	1.259	1.225	**0.194**	0.390	0.344

TABLE 9. Probability of Each Cluster/Label and Information Entropy for Event in WECC

	Frequency event			Voltage event			Oscillation event		
	PMU#850	PMU#209	PMU#864	PMU#992	PMU#789	PMU#641	PMU#641	PMU#789	PMU#193
Probability (label 1)	0.572	0.084	0.536	0.296	0.533	0.862	0.434	0.434	0.000
Probability (label 2)	0.427	0.891	0.452	0.000	0.000	0.000	0.099	0.099	0.000
Probability (label 3)	0.000	0.016	0.011	0.003	0.004	0.003	0.122	0.122	0.999
Probability (label 4)	0.000	0.009	0.002	0.001	0.001	0.001	0.250	0.250	0.000
Probability (label 5)	Not applicable			0.699	0.462	0.134	0.095	0.095	0.001
Information entropy	0.989	0.607	1.089	0.921	1.046	0.610	2.046	2.046	0.009

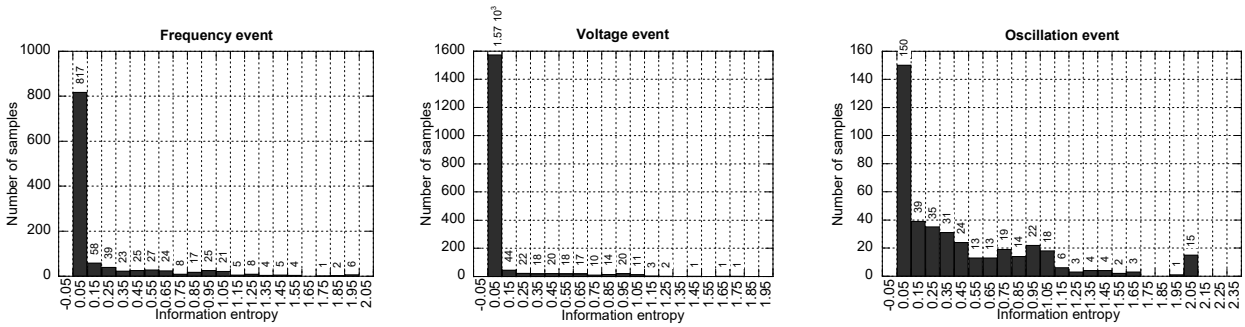

FIGURE 8. Histogram of information entropy with empirical clustering for frequency, voltage, and oscillation events.

C. VISUALIZATION OF LOW-LEVEL EVENT TYPES

According to the empirical label set, all testing signals have been categorized into their assigned low-level event types. These assigned signals and all training signals are combined, then plotted, along with their centroids (red), in the following figures.

1) Frequency Events

Frequency event subclass signatures are plotted in Fig. 9. The event occurs at the 100th time index. The second and third clusters have an immediate drop at this index, whereas the fourth cluster has no such drop. A significant voltage drop at the event start emerges only for the third cluster. Therefore, the cluster centroid at each cluster captures the predominant event signature. Note that the first cluster is the non-event cluster.

The signature of centroid PMUs from frequency events is depicted for each cluster in Fig. 10. The second and third clusters possess the immediate frequency drop, and the second cluster demonstrates the immediate voltage drop. The fourth cluster includes the inter-area oscillation following the event, which is not illustrated in the fourth cluster centroid. Although the first cluster is the non-event cluster, it seems to be a frequency event. However, this must be either a slow frequency change due to gradual generation/load change or a subtle frequency event, such as a 25% dump test of small capacity generators in the bulk power grid.

2) Voltage Events

Each cluster centroid overall represents distinct dynamic voltage behaviors at the 100th time index, especially in terms of voltage dip levels (see Fig. 11). However, the distinction sensitivity to five clusters is not high, especially for the slow voltage recovery characteristics for the subsequent tiny voltage drop in the second cluster. It can be considered that the timing of the subsequent voltage sag is distributed from event to event, which reduces the sensitivity to extracting the distinctive feature.

Fig. 12 displays the selected PMU responses for each cluster as the centroid PMU. The second centroid PMU shows the apparent subsequent tiny voltage dip with the slow voltage recovery. The third centroid PMU represents prominent slow voltage recovery after the voltage dip. The fourth centroid PMU has a significant voltage sag without slow voltage recovery. The fifth centroid PMU expresses the small voltage dip different from the insensible voltage drop with no particular voltage event in the first centroid PMU. It is recognized that all centroid PMU signals properly capture

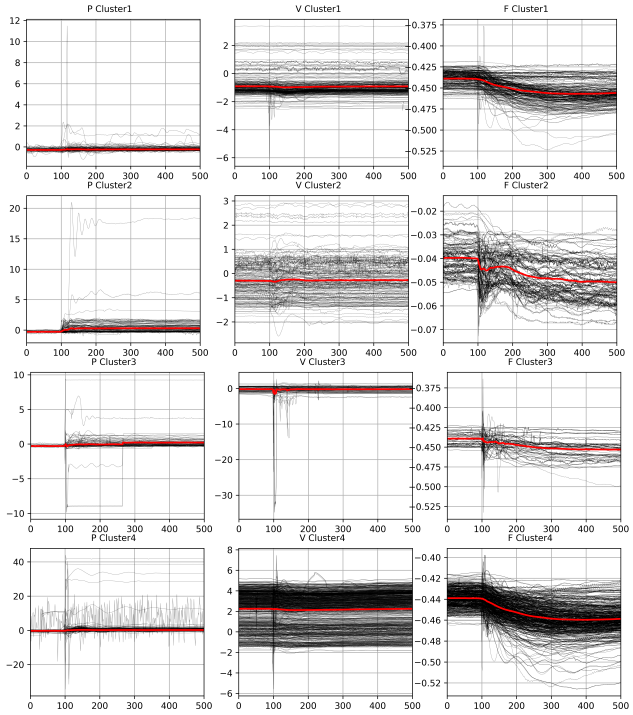

FIGURE 9. Low-level event type centroids for frequency events.

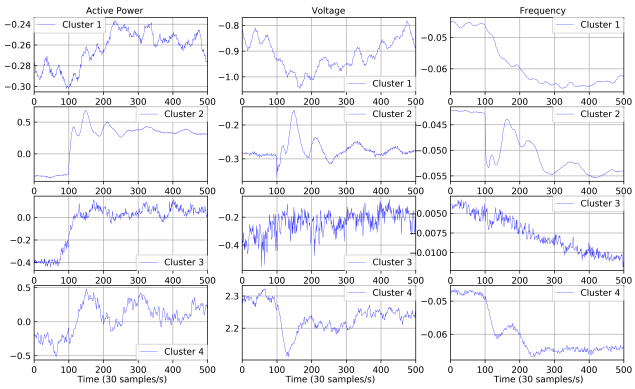

FIGURE 10. Centroid PMU for frequency event.

the distinctive features of dynamic voltage responses.

3) Oscillation Events

Fig. 13 demonstrates all the oscillatory signals that are split into five groups. The second cluster centroid successfully expresses a significant voltage dip. The fraction of high-frequency oscillation components in the third cluster centroid is decidedly higher than that in the first cluster centroid. However, the fourth cluster centroid has no fluctuation that is also observed in the fifth cluster centroid, i.e., non-event signals. The oscillation frequency can be slightly different from sample to sample due to the different power system configurations and conditions. Besides, the phase of oscillatory signals at the time of t is more likely to be equally

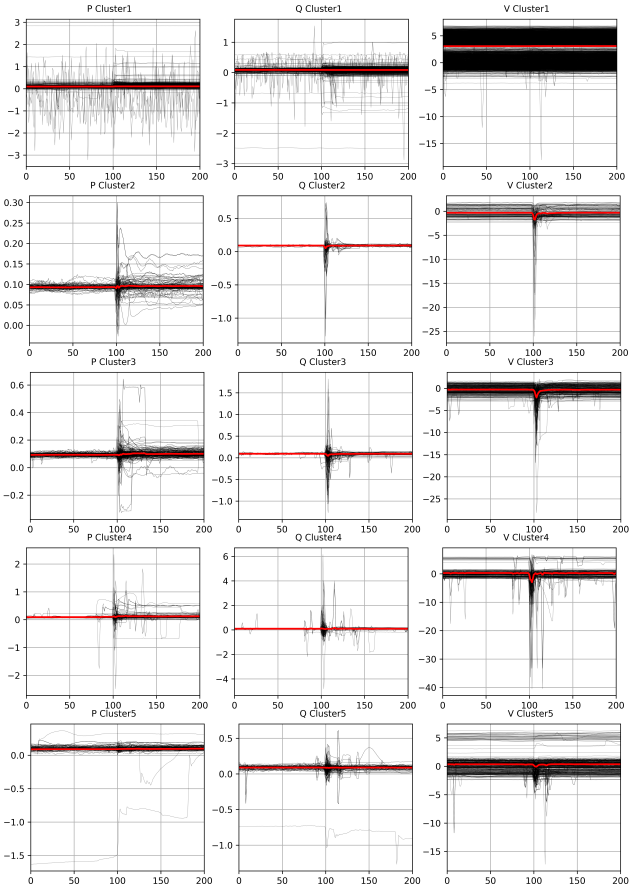

FIGURE 11. Low-level event type centroids for voltage event.

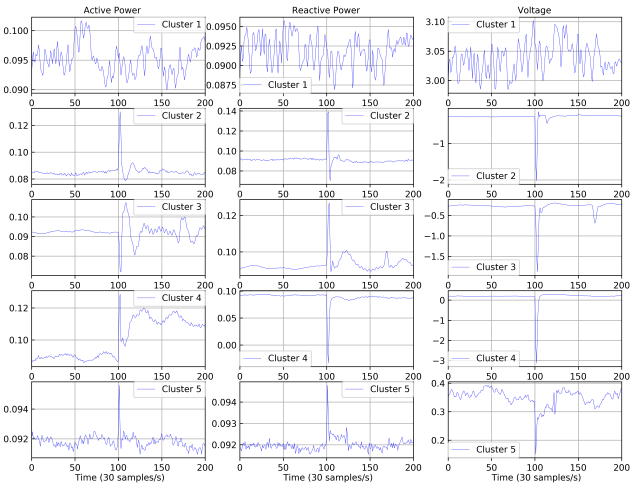

FIGURE 12. Centroid PMU for voltage event.

dispersed as the number of samples increases. Therefore, fluctuated signals must be canceled out when deriving the cluster centroid.

Extracted centroid PMUs are illustrated in Fig. 14. The active and reactive power in the third centroid PMU shows a higher fraction of high-frequency oscillation components

than those in the first centroid PMU. Although the first and fourth voltage centroid PMUs depict similar inter-area oscillation, the first centroid PMU in active and reactive power contains the high-frequency oscillation component. The second centroid PMU possesses a voltage dip much more extensive than that in the third centroid PMU. The non-event centroid PMU, i.e., the fifth centroid PMU successfully displays the white noise with tiny amplitude.

D. NEW EVENT SIGNATURE MINING

As mentioned earlier, the information entropy index is capable of mining unprecedented/new event signatures. This subsection discusses how the event library that is designed explicitly for frequency, voltage, and oscillation events, mines new event signatures, respectively.

1) Frequency Events

The event library for frequency events is leveraged for an event with the high-level label of a frequency event. The historical data is depicted in Fig. 15. Three PMUs that include apparent frequency drops are only showcased in this figure for their visibility. It can be seen from Table 9 that the first and second clusters show a high probability. Specifically, PMU 850 and PMU 864 have nearly the same probabilities for label 1 and label 2. Besides, the information entropy is incredibly high (Note that most information entropy is less than 0.1, as shown in Fig. 8).

The event timing is set at 20 s in Fig. 15. The first cluster stands for non-event and the second cluster corresponds to the frequency drop with frequency transients (see Table 2). However, it is tangible that no signals possess the frequency drop and frequency transient. On the contrary, the frequency rise is obviously observed until 27 s, which is quite rare in frequency events that TSOs/RTOs picked and has been out-of-scope for manually labeled frequency events in Table 2. Therefore, frequency rise events should be recognized as an unprecedented or non-categorized event with high information entropy.

2) Voltage Events

The event library for voltage events is used for an event with the high-level label of a line event that is generally treated as a voltage event. The historical data is depicted in Fig. 15, limiting PMUs with significant voltage dip to three for its presentability. The line tripping event occurred at the time of 20 s and the system frequency started to decline. Due to the conspicuous frequency drop signature, it is evident that a generator tripping/disconnection had occurred along with the line tripping event. The predetermined labels in Table 3 do not include the combined voltage and frequency event because frequency events are not supposed to be missed in the high-level frequency label, i.e., frequency events can never be categorized in events labeled as voltage events. Then, frequency signals are skipped for the voltage event (See Table 5). It is emphasized that the event library can identify frequency events as the uncategorized voltage event

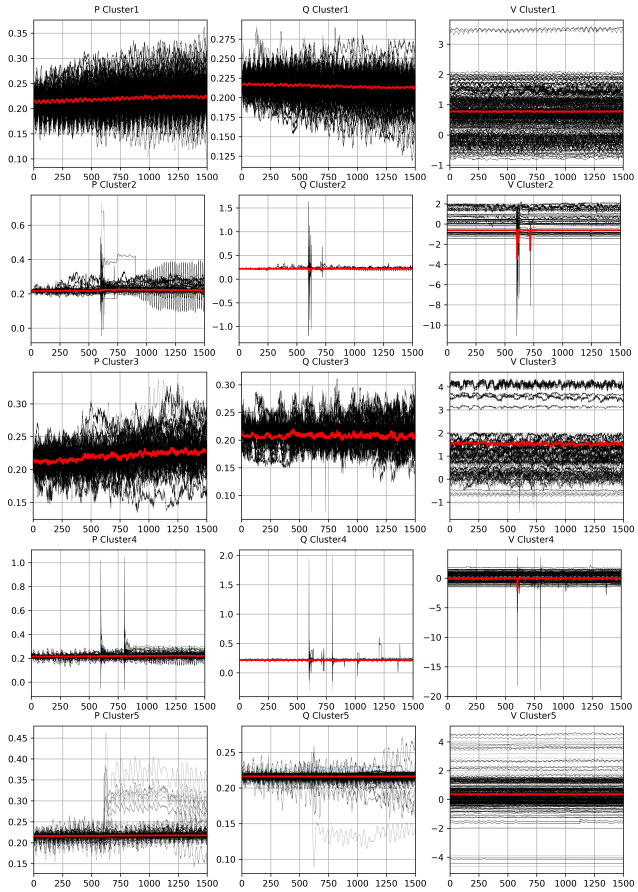

FIGURE 13. Low-level event type centroids for oscillation event.

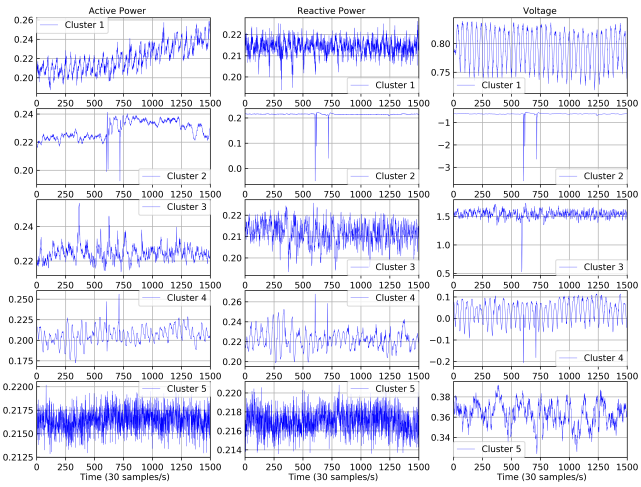

FIGURE 14. Centroid PMU for oscillation event.

without frequency signals, i.e., with active power, reactive power, and voltage signals only.

Each probability and information entropy are summarized for the three PMUs in Table 9. The first cluster and the fifth cluster show a high probability. Besides, the information entropy ranges from 0.6-1.0 that correspond to the 96-99th

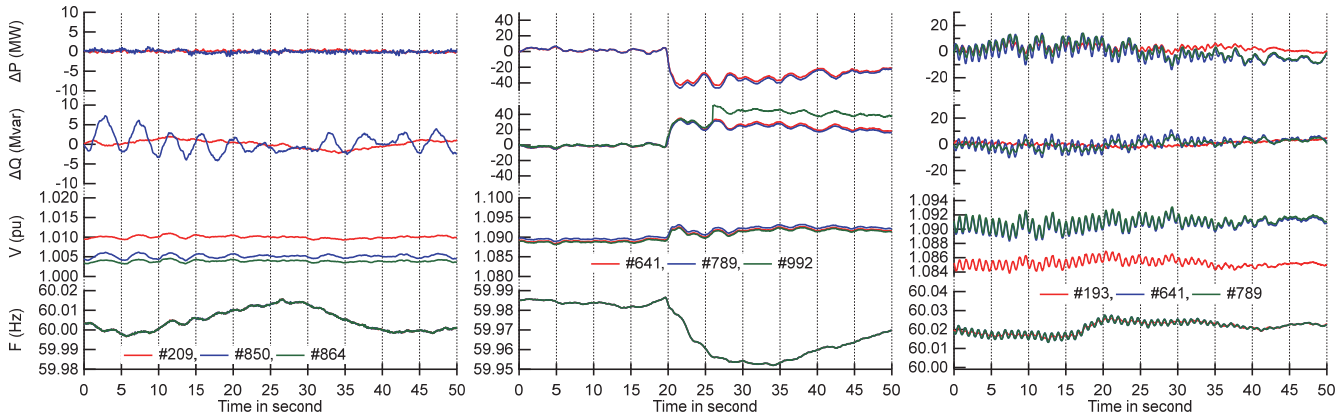

(a) Frequency (rise) event (b) Voltage (line tripping) event (c) Oscillation event

FIGURE 15. Example of unprecedented event signatures the event timing of which is 20 s for frequency and voltage events.

percentiles of Fig. 8. Thus, this mixture of voltage and frequency events may be recognized as an unprecedented or non-categorized event with high information entropy.

3) Oscillation Events

The event library for an oscillation event is used for a representative oscillation event. The recorded data is demonstrated in Fig. 15, highlighting three PMUs that have distinct oscillations. The characteristics of this event can be curated as gradually disappearing high-frequency oscillations.

Each probability and information entropy are presented for the representative 3 PMUs in Table 9. It is noted that the PNNL randomly assigned 43 PMU IDs in the WECC in the range of 100 and 999 for security reasons. The first and the fourth clusters show a high probability for PMU 641 and PMU 749. Besides, the information entropy is extraordinarily high, which corresponds to the 96th percentile in Fig. 8. As shown in Table 4, the first label corresponds to an oscillation with low and high-frequency components, whereas the fourth label contains only low-frequency components in the oscillatory signals. PMU 641 and PMU 789 include two signatures:

1) Oscillation with high and low-frequency components (before 137 s)
2) Oscillation with low-frequency components only (after 137 s)

Therefore, it is seen that PMU 641 and PMU 789 have a significant probability for both label 1 and label 4 in Table 4. Table 9 also demonstrates a similar event signature of PMU 193. Although the frequency signal is entirely the same as those in PMU 641 and PMU 789, the low-frequency oscillation is not involved in the active power, reactive power, and voltage of PMU 193. Because slight fluctuations remain even after 137 s, PMU 193 has a specific label 3 with small information entropy, as shown in Table 9.

4) Requirements for Additional Labels

A new category constantly enlarges the information entropy. On the other hand, an event with large information entropy does not always indicate that a new category is requested. For example, the large information entropy can also indicate the mixture of two different signatures at distinct periods. Therefore, further investigation is required to add one more label. Also, a sufficient number of samples is vital to insert the new label. Whenever a new label is showcased, the ResNet-50 V2 model will be re-trained.

V. FUTURE WORK

The event signature library design was individually crafted for frequency events, voltage events, and oscillation events. Properly selecting electric quantities with manually-created labels improved the selectivity of each event signature category/label. Newly added small category labels (i.e., low-level labels) are based on expert reviews of over 1000 real events in the bulk U.S. power grid. The low-level labels are carefully distilled, considering remarkable features for each event type. The classifier with empirical labels exhibits nearly half of the information entropy on average compared to the classifier with automatic labels.

The Eastern Interconnection event data was used for training the model. The WECC event data was employed for testing the model. Because the established event signature library design not only successfully trained but properly validated the model, the developed design shows outstanding performance for the two different interconnections.

A simple but effective single indicator is devised, using the information entropy to confirm whether the identified event signature category is clear or not, and to find unprecedented event signatures effectively. Newly obtained lower-level (small category) labels from the event signature library would be paramount for future data-driven research studies in academia as well as for the power engineers at the control centers.

Although the prototype of the event signature library has been successfully created, there is room for further refinement shown below:

- Frequency rise due to load change, including pumped storage unit tripping under the pumping mode
- Multiple (more than two) subsequent voltage drops
- Distinction between local oscillations and converter-driven oscillations
- Distinction between ringdown oscillations and growing oscillations towards out-of-step (including poorly damped or sustained oscillations)

Specifically, increasing penetration of renewable energies must augment the frequency of converter-driven oscillation events. Currently, the number of available data with the converter-driven oscillation is insufficient and needs to be accumulated to generate the classifier module.

The lower thresholds shown in Table 1 are also indicated with blue arrows.

VI. ACKNOWLEDGMENTS

This material is based upon work supported by the Department of Energy under Award Number DE-0000916.

REFERENCES

[1] N. Hatziargyriou, J. Milanovic, C. Rahmann, V. Ajjarapu, C. Canizares, I. Erlich, D. Hill, I. Hiskens, I. Kamwa, B. Pal, P. Pourbeik, J. Sanchez-Gasca, A. Stankovic, T. V. Cutsem, V. Vittal, and C. Vournas, "Definition and classification of power system stability - revisited & extended," *IEEE Trans. Power Syst.*, vol. 36, no. 4, 2021.

[2] ENTSO-E, "Incident classification scale methodology," Dec. 2019, Accessed: Sep. 5, 2022. [Online]. Available: https://eepublicdownloads.entsoe.eu/clean-documents/SOCdocuments/Incident_Classification_Scale/IN_USE_FROM_JANUARY_2020_191204_Incident_Classification_Scale.pdf

[3] *Event Reporting*, NERC Std. EOP-004-4, Nov. 2018. [Online]. Available: https://www.nerc.com/pa/Stand/ReliabilityStandards/EOP-004-4.pdf

[4] A. Phadke, "Synchronized phasor measurements in power systems," *IEEE Trans. Power Syst.*, vol. 6, no. 2, pp. 1914–1921, Apr. 1993.

[5] J. E. Tate and T. J. Overbye, "Line outage detection using phasor angle measurements," *IEEE Trans. Power Syst.*, vol. 23, no. 4, pp. 1644 – 1652, Nov. 2008.

[6] Z. Zhong, C. Xu, B. Billian, L. Zhang, S.-J. Tsai, R. Conners, V. Centeno, A. Phadke, and Y. Liu, "Power system frequency monitoring network (FNET) implementation," *IEEE Trans. Power Syst.*, vol. 20, no. 4, pp. 1914–1921, Nov. 2005.

[7] M. Moreto, J. G. Rolim, and F. S. Varela, "Automating the diagnosis of occurrences in power plants using data from DFR and sequence of events: an expert system based methodology," in *Proc. 15th Int. Conf. on Intelligent System Applications to Power Systems*, Nov. 2009.

[8] NERC, "Eastern interconnection oscillation disturbance january 11, 2019 forced oscillation event," NERC, Disturbance Report, Dec. 2019, Accessed: Sep. 5, 2022. [Online]. Available: https://www.nerc.com/pa/rrm/ea/Documents/January_11_Oscillation_Event_Report.pdf

[9] B. Wang and K. Sun, "Location methods of oscillation sources in power systems: a survey," *J. Mod. Power Syst. Clean Energy*, vol. 5, no. 2, pp. 151 – 159, Mar. 2017.

[10] Y. Ge, A. J. Flueck, D.-K. Kim, J.-B. Ahn, J.-D. Lee, and D.-Y. Kwon, "Power system real-time event detection and associated data archival reduction based on synchrophasors," *IEEE Trans. Smart Grid*, vol. 6, no. 4, pp. 2088–2097, 2015.

[11] W. Wang, H. Yin, C. Chen, A. Till, W. Yao, X. Deng, and Y. Liu, "Frequency disturbance event detection based on synchrophasors and deep learning," *IEEE Trans. Smart Grid*, vol. 11, no. 4, pp. 3593–3605, 2020.

[12] J. Shi, B. Foggo, and N. Yu, "Power system event identification based on deep neural network with information loading," *IEEE Trans. Power Syst.*, vol. 36, no. 6, pp. 5622–5632, Nov. 2021.

[13] S. Liu, Y. Zhao, Z. Lin, Y. Liu, Y. Ding, L. Yang, and S. Yi, "Data-driven event detection of power systems based on unequal-interval reduction of PMU data and local outlier factor," *IEEE Trans. Smart Grid*, vol. 11, no. 2, pp. 1630–1643, 2020.

[14] O. P. Dahal and S. M. Brahma, "Preliminary work to classify the disturbance events recorded by phasor measurement units," in *2012 IEEE Power and Energy Society General Meeting*, Jul. 2012, pp. 1–8.

[15] V. Miranda, P. A. Cardoso, R. J. Bessa, and I. Decker, "Through the looking glass: Seeing events in power systems dynamics," *Int. J. Electr. Power Energy Syst.*, vol. 106, pp. 411 – 419, 2019.

[16] M. Biswal, S. M. Brahma, and H. Cao, "Supervisory protection and automated event diagnosis using PMU data," *IEEE Trans. Power Del.*, vol. 31, no. 4, pp. 1855–1863, 2016.

[17] Y. Song, W. Wang, Z. Zhang, H. Qi, and Y. Liu, "Multiple event detection and recognition for large-scale power systems through clusterbased sparse coding," *IEEE Trans. Power Syst.*, vol. 32, no. 6, pp. 4199–4210, 2017.

[18] W. W. Ng, J. Zhang, C. S. Lai, W. Pedrycz, L. L. Lai, and X. Wang, "Cost-sensitive weighting and imbalance-reversed bagging for streaming imbalanced and concept drifting in electricity pricing classification," *IEEE Trans. Ind. Informat.*, vol. 15, no. 3, pp. 1588–1597, 2018.

[19] Y. Song, W. Wang, Z. Zhang, H. Qi, and Y. Liu, "Real-time event classification in power system with renewables using kernel density estimation and deep neural network," *IEEE Trans. Smart Grid*, vol. 10, no. 6, pp. 6849–6859, 2019.

[20] W. Li and M. Wang, "Identifying overlapping successive events using a shallow convolutional neural network," *IEEE Trans. Power Syst.*, vol. 34, no. 6, pp. 4762–4772, 2019.

[21] W. Wang, L. He, P. Markham, H. Qi, Y. Liu, Q. C. Cao, and L. M. Tolbert, "Multiple event detection and recognition through sparse unmixing for high-resolution situational awareness in power grid," *IEEE Trans. Smart Grid*, vol. 5, no. 4, pp. 1654–1664, 2014.

[22] M. Rafferty, X. Liu, D. M. Laverty, and S. McLoone, "Real-time multiple event detection and classification using moving window pca," *IEEE Trans. Smart Grid*, vol. 7, no. 5, pp. 2537–2548, 2016.

[23] R. Yadav, A. K. Pradhan, and I. Kamwa, "Real-time multiple event detection and classification in power system using signal energy transformations," *IEEE Trans. Ind. Informat.*, vol. 15, no. 3, pp. 1521–1531, 2018.

[24] A. F. Bastos and S. Santoso, "Universal waveshape-based disturbance detection in power quality data using similarity metrics," *IEEE Trans. Power Del.*, vol. 35, no. 4, pp. 1779–1787, 2019.

[25] F. Yang, M. Wei, Z. Ling, T. Mi, H. Yang, and R. C. Qiu, "Brown measure based spectral distribution analysis for spatial-temporal localization of cascading events in power grids," *IEEE Trans. Smart Grid*, vol. 12, no. 3, pp. 1805–1820, 2021.

[26] A. Ahmed, K. Sajan, A. Srivastava, and Y. Wu, "Anomaly detection, localization and classification using drifting synchrophasor data streams," *IEEE Trans. Smart Grid*, vol. 12, no. 4, pp. 3570–3580, 2021.

[27] S. Pandey, A. K. Srivastava, and B. G. Amidan, "A real time event detection, classification and localization using synchrophasor data," *IEEE Trans. Power Syst.*, vol. 35, no. 6, pp. 4421–4431, 2020.

[28] A. Vosughi, K. S. Sajan, and A. Srivastava, "Synchrophasor-based event detection, classification and localization using koopman, transient energy matrix, best worth method, and dynamic graph," *IEEE Trans. Power Del.*, vol. 37, no. 3, pp. 1986–1996, Jun. 2022.

[29] K. B. Swain, S. S. Mahato, and M. Cherukuri, "Expeditious situational awareness-based transmission line fault classification and prediction using synchronized phasor measurements," *IEEE Access*, vol. 7, pp. 168 187–168 200, 2019.

[30] D.-I. Kim, L. Wang, and Y.-J. Shin, "Data driven method for event classification via regional segmentation of power systems," *IEEE Access*, vol. 8, pp. 48 195–48 204, 2020.

[31] X. Zheng, B. Wang, D. Kalathil, and L. Xie, "Generative adversarial networks-based synthetic PMU data creation for improved event classification," *IEEE open access j. power energy*, vol. 8, pp. 68–76, 2021.

[32] J. S. Banning, J. D. Follum, and E. S. Andersen, "FOA 1861 data curation overview," PNNL, Tech. Rep. PNNL-32303, Oct. 2021, Accessed: Sep. 5, 2022. [Online]. Available: https://www.osti.gov/biblio/1860940

[33] NASPI PMU Applications Requirements Task Force, "PMU data quality: A framework for the attributes of PMU data quality and a methodology for examining data quality impacts to synchrophasor applications," NASPI, NASPI-2017-TR-002/ PNNL-26313, Mar. 2017, Accessed: Sep. 5, 2022. [Online]. Available: https://www.naspi.org/node/352

[34] B. P. Leao, D. Fradkin, Y. Wang, and S. Suresh, "Big data processing for power grid event detection," in *Proc. of 2020 IEEE Int. Conf. on Big Data*, Dec. 2020, doi:10.1109/BigData50022.2020.9378106.

[35] S. Barratt and R. Sharma, "A note on the inception score," *arXiv preprint arXiv:1801.01973*, 2018.

[36] U.S. Department of Energy, "Electric disturbance events (DOE-417)," May 2018, Accessed: Sep. 5, 2022. [Online]. Available: https://www.oe.netl.doe.gov/oe417.aspx

[37] P. Gao, M. Wang, S. G. Ghiocel, J. H. Chow, B. Fardanesh, and G. Stefopoulos, "Missing data recovery by exploiting low-dimensionality in power system synchrophasor measurements," *IEEE Trans. Power Syst.*, vol. 31, no. 2, pp. 1006–1013, 2016.

[38] W.-T. Li, C.-K. Wen, J.-C. Chen, K.-K. Wong, J.-H. Teng, and C. Yuen, "Location identification of power line outages using PMU measurements with bad data," *IEEE Trans. Power Syst.*, vol. 31, no. 5, pp. 3624 – 3635, Sep. 2016.

[39] California ISO and West RC, "Reliability coordinator procedure -event reporting," Apr. 2020, Accessed: Sep. 5, 2022. [Online]. Available: https://www.caiso.com/Documents/RC0420.pdf

[40] NERC, "San Fernando disturbance - southern California event: July 7, 2020," NERC, Joint NERC and WECC Staff Report, Nov. 2020, Accessed: Sep. 5, 2022. [Online]. Available: https://www.nerc.com/pa/rrm/ea/Documents/San_Fernando_Disturbance_Report.pdf

[41] J. Paparrizos and L. Gravano, "K-shape: Efficient and accurate clustering of time series," *ACM SIGMOD Record*, vol. 45, pp. 69–76, Jun. 2016.

[42] B. Leao, "Mind synchro -FOA 1861," in *NASPI Work Group Virtual Meeting and Vendor Show*, Oct. 2021, Accessed: Sep. 5, 2022. [Online]. Available: https://www.naspi.org/sites/default/files/2021-10/D1S1_05_leao_siemens_20211005.pdf

[43] NERC, "Lesson learned -interconnection oscillation disturbances," May 2021, Accessed: Sep. 5, 2022. [Online]. Available: https://www.nerc.com/pa/rrm/ea/LessonsLearnedDocumentLibrary/LL20210501_Interconnection_Oscillation_Disturbances.pdf

[44] NERC, "Interconnection oscillation analysis," NERC, Reliability Assessment, July 2019, Accessed: Sep. 5, 2022. [Online]. Available: https://www.nerc.com/comm/PC/SMSResourcesDocuments/Interconnection_Oscillation_Analysis.pdf

[45] X. Zheng, B. Wang, and L. Xie, "Synthetic dynamic PMU data generation: A generative adversarial network approach," in *Proc. 2019 Int. Conf. on Smart Grid Synchronized Measurements and Analytics (SGSMA)*, Oct.-Nov. 2019, doi: 10.1109/SGSMA.2019.8784681.

[46] K. He, X. Zhang, S. Ren, and J. Sun, "Deep residual learning for image recognition," in *Proc. the IEEE Conf. on Computer Vision and Pattern Recognition (CVPR)*, Jun. 2016, doi: 10.1109/CVPR.2016.90.

[47] H. Sakoe and S. Chiba, "Dynamic programming algorithm optimization for spoken word recognition," *IEEE Trans. Acoust., Speech, Signal Process.*, vol. 26, no. 1, pp. 43–49, 1978.

KOJI YAMASHITA (M'04) received his B.S. and M.S. degrees in Electrical Engineering from Waseda University, Tokyo, Japan, in 1993 and 1995, respectively. He also received his Ph.D. degree in Electrical and Computer Engineering from Michigan Technological University, Houghton, MI, USA, in 2020. He was a research scientist with the power system division of CRIEPI, Japan, from 1995–2018. He is currently a postdoctoral scholar at the University of California Riverside, cultivating machine learning techniques for power system dynamics. His research interests are power system dynamic performance and its modeling.

BRANDON FOGGO (M'19) received a B.S. degree in Electrical Engineering from the University of California, Los Angeles, in 2015, and a Ph.D. degree in Electrical and Computer Engineering from the University of California, Riverside, in 2019. His research interests lie in statistical learning theory and information theory, particularly in their merging, as well as applications to cyber physical systems with an emphasis on power distribution systems.

XIANGHAO KONG received a B.S. degree in Computer Science from Hangzhou Dianzi University, Hangzhou, China, in 2019. He is now pursuing his Ph.D. degree in Computer Science from the University of California, Riverside, CA, USA. His research interests lie in time-efficient machine learning and big data analysis in dynamic systems.

YUANBIN CHENG received a B.S. degree in Computer Science from the University of Science and Technology of China, Anhui, China, in 2016. He received his M.S. degree in Computer Science from the University of Southern California, CA, USA, in 2018. He is now pursuing his Ph.D. degree in Computer Science from the University of California, Riverside. His research interests lie in various deep learning algorithms for big data analysis in dynamic systems.

JIE SHI (M'21) received a B.S. degree in Automation from Shenyang University of Technology, Shenyang, China, in 2012. He received an M.S. degree in Control Theory & Control Engineering from Southeast University, Nanjing, China, in 2015. He received his Ph.D. degree in Electrical and Computer Engineering from the University of California, Riverside, CA, USA, in 2021. He was a postdoctoral researcher in Systems Engineering at Cornell University. His research interests include smart infrastructure systems, intelligent systems, and machine learning.

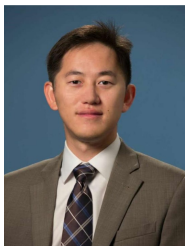

NANPENG YU (M'11-SM'16) received his B.S. in Electrical Engineering from Tsinghua University, Beijing, China, in 2006. Dr. Yu also received his M.S. and Ph.D. degrees in Electrical Engineering from Iowa State University, Ames, IA, USA, in 2007 and 2010, respectively. He is currently an Associate Professor in the Department of Electrical and Computer Engineering at the University of California, Riverside, CA, USA. His current research interests include machine learning in smart grid, electricity market design and optimization, and smart energy communities. Dr. Yu is an Editor of IEEE Transactions on Smart Grid and IEEE Transactions on Sustainable Energy.